1972

Numerical integration experiments with a barotropic primitive equation model.

Slaughter, Jimmy Ray.

Monterey, California. Naval Postgraduate School

NUMERICAL INTEGRATION EXPERIMENTS WITH A BAROTROPIC PRIMITIVE EQUATION MODEL

Jimmy Ray Slaughter

NAVAL POSTGRADUATE SCHOOL
Monterey, California

THESIS

Numerical Integration Experiments With
a
Barotropic Primitive Equation Model

by

Jimmy Ray Slaughter

Thesis Advisor G. J. Haltiner

March 1972

Numerical Integration Experiments With
a
Barotropic Primitive Equation Model

by

Jimmy Ray Slaughter
Lieutenant Commander, United States Navy
B.S., United States Naval Academy, 1963

Submitted in partial fulfillment of the
requirements for the degree of

MASTER OF SCIENCE IN METEOROLOGY

from the

NAVAL POSTGRADUATE SCHOOL
March 1972

ABSTRACT

Experiments are carried out with various time and space differencing schemes applied to the barotropic primitive equations using both real data and a particular stream function which is an analytic solution to the nondivergent barotropic vorticity equation. With both types of data, there were some significant differences in the forecasts produced by the various schemes. Replacement of the widely used leap frog (centered) scheme by others which eliminate or lessen some of its inherent errors at the expense of more computer time or storage appears to be justified at such time when computer capacity no longer restricts operational use of these more time consuming schemes.

TABLE OF CONTENTS

LIST OF TABLES

LIST OF FIGURES

LIST OF SYMBOLS

c	Phase speed.
d	Grid distance.
d'	Grid distance at 60 degrees latitude.
f	Coriolis parameter.
$\bar{f}$	Coriolis parameter at 60 degrees latitude.
FNWC	Fleet Numerical Weather Central.
g	Force of gravity.
h	Height of meteorological surface.
L_x	Wavelength in the x direction.
L_y	Half a wavelength in the y direction.
m	Map factor.
u	Velocity component in the x direction.
v	Velocity component in the y direction.
v_o	Initial meridional wind speed.
α	Relaxation coefficient.
ζ	Relative vorticity.
ϕ	Geopotential.
ψ	Stream function.
ψ_o	Initial stream function amplitude.

I. INTRODUCTION

In selecting a particular differencing scheme for application to numerical weather prediction, a major consideration is computer time and storage requirements. Therefore, the selected scheme is a compromise between verification accuracy and computer limitations. At present, the leap frog (centered) scheme is widely used in numerical weather prediction and will be used as a standard for purposes of comparison. Present computer limitations and methods of verification tend to preclude seeking more accurate solutions based on mathematical considerations alone. The purpose of this study is to look beyond present computer capabilities and examine several other differencing schemes which reduce or eliminate some of the inaccuracies in the leap frog scheme. This scheme has three time levels and, therefore, a spurious computational mode arises from the finite differencing scheme. This problem can be eliminated by the application of two level time schemes such as the Euler backward or Runge Kutta methods which have on computational mode. A fourth order space differencing scheme is applied to reduce truncation error and improve phase speeds. Should any of the schemes produce a significant change in forecast relative to the leap frog method, it must be determined if the difference represents a sufficient increase in accuracy to warrant the added computer time and storage requirements.

II. PROGNOSTIC EQUATIONS

The equations of motion and the continuity equation for a barotropic fluid in the momentum flux form are

$$\frac{\partial(uh)}{\partial t} + m^2\frac{\partial}{\partial x}\left(\frac{uuh}{m}\right) + m^2\frac{\partial}{\partial y}\left(\frac{uvh}{m}\right) - \frac{fvh}{} = -mgh\frac{\partial h}{\partial x} \tag{1}$$

$$\frac{\partial(vh)}{\partial t} + m^2\frac{\partial}{\partial x}\left(\frac{vuh}{m}\right) + m^2\frac{\partial}{\partial y}\left(\frac{vvh}{m}\right) + \frac{fuh}{} = -mgh\frac{\partial h}{\partial y} \tag{2}$$

$$\frac{\partial h}{\partial t} + m^2\left[\frac{\partial}{\partial x}\frac{(uh)}{m} + \frac{\partial}{\partial y}\frac{(vh)}{m}\right] = 0 \tag{3}$$

where h is the depth of the fluid (or height of a pressure surface in the atmosphere), g is the force of gravity, f is the coriolis parameter and u and v are horizontal velocity components.

A. SPACE DIFFERENCING

1. Second Order Scheme

With u, v, and h given at each grid point, the differential equations may be approximated by

$$\begin{aligned}\frac{\partial}{\partial t}\left(\frac{uh}{}\right)_{ij} = -m^2/4d[&(u_{i+1,j} + u_{ij})\left(\frac{uh_{i+1,j}}{m} + \frac{uh_{ij}}{m}\right)\\ &- (u_{i-1,j} + u_{ij})\left(\frac{uh_{i-1,j}}{m} + \frac{uh_{ij}}{m}\right)\\ &+ (u_{i,j+1} + u_{ij})\left(\frac{vh_{i,j+1}}{m} + \frac{vh_{ij}}{m}\right)\\ &- (u_{i,j-1} + u_{ij})\left(\frac{vh_{i,j-1}}{m} + \frac{vh_{ij}}{m}\right)] + f_{ij}(vh)_{ij}\\ &- mgh_{ij}(h_{i+1,j} - h_{i-1,j})/2d \equiv F_{ij}\end{aligned} \tag{4}$$

where j increases with x and i decreases with y. (See Fig. 1) Similar expressions are used for the other two equa-

tions. This method of space differencing, devised by A. Arakawa (see, for example, [1]), prevents nonlinear instability in the continuous time case (sometimes referred to as the semi-discrete equations).

2. Fourth Order Scheme

Fourth order space differencing which takes into account a greater number of grid points and reduces truncation error approximates uh tendencies by

$$\frac{\partial}{\partial t}\frac{(uh)}{}_{i,j} = 4/3(F_{ij}) - \frac{1}{3}\Big\{-\frac{m^2}{8d}\big[(u_{i+2,j}+u_{ij})(\frac{uh}{m}_{i+2,j} + \frac{uh}{m}_{i,j}) - (u_{i-2,j}+u_{ij})(\frac{uh}{m}_{i-2,j}+\frac{uh}{m}_{ij})$$
$$+(u_{i,j+2}+u_{ij})(\frac{vh}{m}_{i,j+2}+\frac{vh}{m}_{ij})$$
$$-(u_{i,j-2}+u_{ij})(\frac{vh}{m}_{i,j-2}+\frac{vh}{m}_{ij})\big] + f_{ij}(vh)_{ij}$$
$$-mgh_{ij}(h_{i+2,j} - h_{i-2,j})/4d\Big\} \qquad (5)$$

where $F_{i,j}$ is the second order space difference.

B. TIME DIFFERENCING

U represents uh, vh, or h; t is time; n is time step number and F is $\frac{\partial U}{\partial t}$ in the following time differencing schemes:

1. Leap Frog

$$U^{n+1} - U^{n-1} = 2\Delta t F^n$$

2. Runge Kutta

$$\Delta U_1 = \Delta t\ F[U^n,\ n\Delta t]$$

$$\Delta U_2 = \Delta t\ F[U^n + \Delta U_1/2,\ (n+\tfrac{1}{2})\Delta t]$$

$$\Delta U_3 = \Delta t \; F[U^n + \frac{\Delta U_2}{2} \; , \; (n + \tfrac{1}{2}) \; \Delta t]$$

$$\Delta U_4 = \Delta t \; F[U^n + \Delta U_3 \; , \; (n + 1) \; \Delta t]$$

$$U^{n+1} = U^n + \tfrac{1}{6}[\Delta U_1 + 2\Delta U_2 + 2\Delta U_3 + \Delta U_4]$$

3. Euler Backward

$$U^* - U^n = \Delta t \; F^n$$

$$U^{n+1} - U^n = \Delta t \; F^*$$

*Denotes trial values.

III. BOUNDARY CONDITIONS

A. A PARTICULAR STREAM FUNCTION

The boundary conditions in this case are applied to an initial stream function which is an analytic solution to the nondivergent barotropic vorticity equation and after each time step during the forecast.

1. North-South Boundary Conditions

For the 63x63 grid a wall exists between y=1 and y=2 and also between y=63 and y=62 (See Fig. 1). No flux is permitted across this rigid boundary. This is accomplished by setting $v_{x,63} = -v_{x,62}$ and $v_{x,1} = -v_{x,2}$ thereby making the average $v_{x,y} = 0$ along the wall. The other parameters are set equal across the wall. Summarizing, the boundary conditions are

North	South
$v_{x,63} = -v_{x,62}$	$v_{x,1} = -v_{x,2}$
$u_{x,63} = u_{x,62}$	$u_{x,1} = u_{x,2}$
$\phi_{x,63} = \phi_{x,62}$	$\phi_{x,1} = \phi_{x,2}$

where ϕ is the geopotential.

2. East-West Boundary Conditions

The East-West boundary conditions are cyclic as suggested by the function plotted in Fig. 1. Summarizing, the boundary conditions are

East	West
$A_{1,y} = A_{62,y}$	$A_{63,y} = A_{2,y}$

where A represents parameters $v_{x,y}$, $u_{x,y}$ and $\phi_{x,y}$.

3. Variation for Fourth Order Space Difference

In order to apply fourth order space differencing and still maintain the boundary conditions of the original grid, it was convenient to create an additional outside row of points and relabel as a 65x65 grid. (See Fig. 2) The boundary conditions are summarized as follows:

North	South	
$v_{x,65} = -v_{x,62}$	$v_{x,1} = -v_{x,4}$	$A_{x,y}$ represents $u_{x,y}$, and $\phi_{x,y}$.
$v_{x,64} = -v_{x,63}$	$v_{x,2} = -v_{x,3}$	
$A_{x,65} = A_{x,62}$	$A_{x,1} = A_{x,4}$	
$A_{x,54} = A_{x,63}$	$A_{x,2} = A_{x,3}$	
East	**West**	
$A_{1,y} = A_{62,y}$	$A_{65,y} = A_{4,y}$	$A_{x,y}$ represents $u_{x,y}$, $v_{x,y}$, and $\phi_{x,y}$.
$A_{2,y} = A_{63,y}$	$A_{64,y} = A_{3,y}$	

B, ACTUAL 500 MILLIBAR DATA

When the equations were integrated using real data, the "spongy" boundary conditions of the FNWC model were applied. After each time step, the prognostic results were modified by setting

$$\underline{uh} = (1-k')\underline{uh} + k' \underline{uh}_o$$

$$\underline{vh} = (1-k')\underline{vh} + k' \underline{vh}_o$$

$$h = (1-k')h + k' h_o$$

where the $_o$ subscript indicates initial values. Below latitude four degrees north set k'=4. Above 17 degrees north set k'=0. Between four degrees north and 17 degrees north, there is linear variation in k' from zero to one. This restores the variables to their initial values south of four degrees north, while north of 17 degrees north, full variability is permitted. There is no restoration north of 17 degrees north. Between, there is partial restoration.

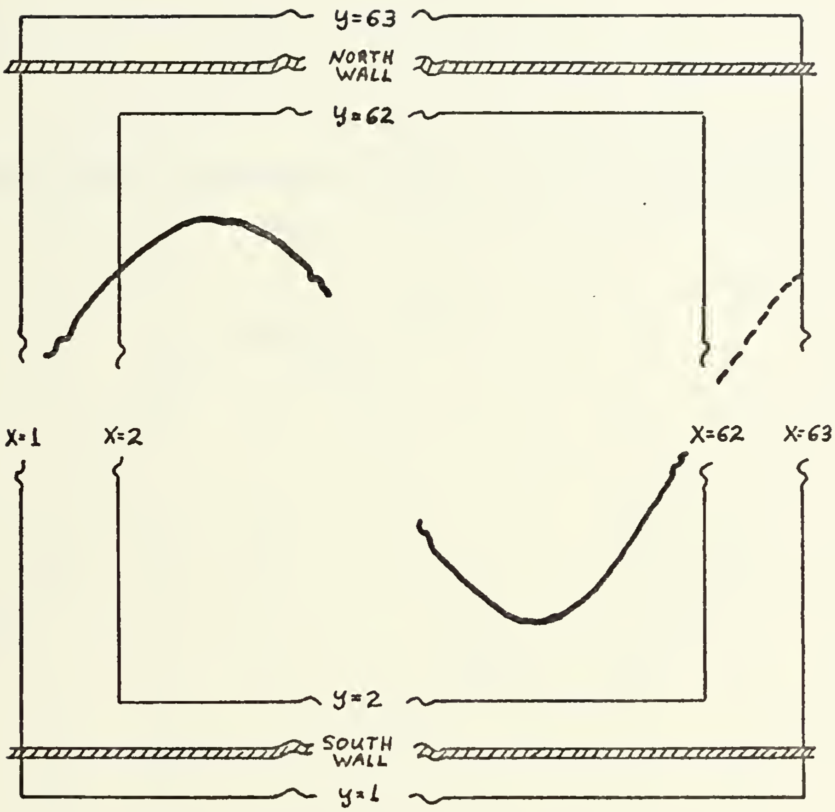

Illustrating the 63x63 square grid and boundaries as applied to a particular stream function. The dimensionless symbols x and y are used for notation convenience.

Figure 1

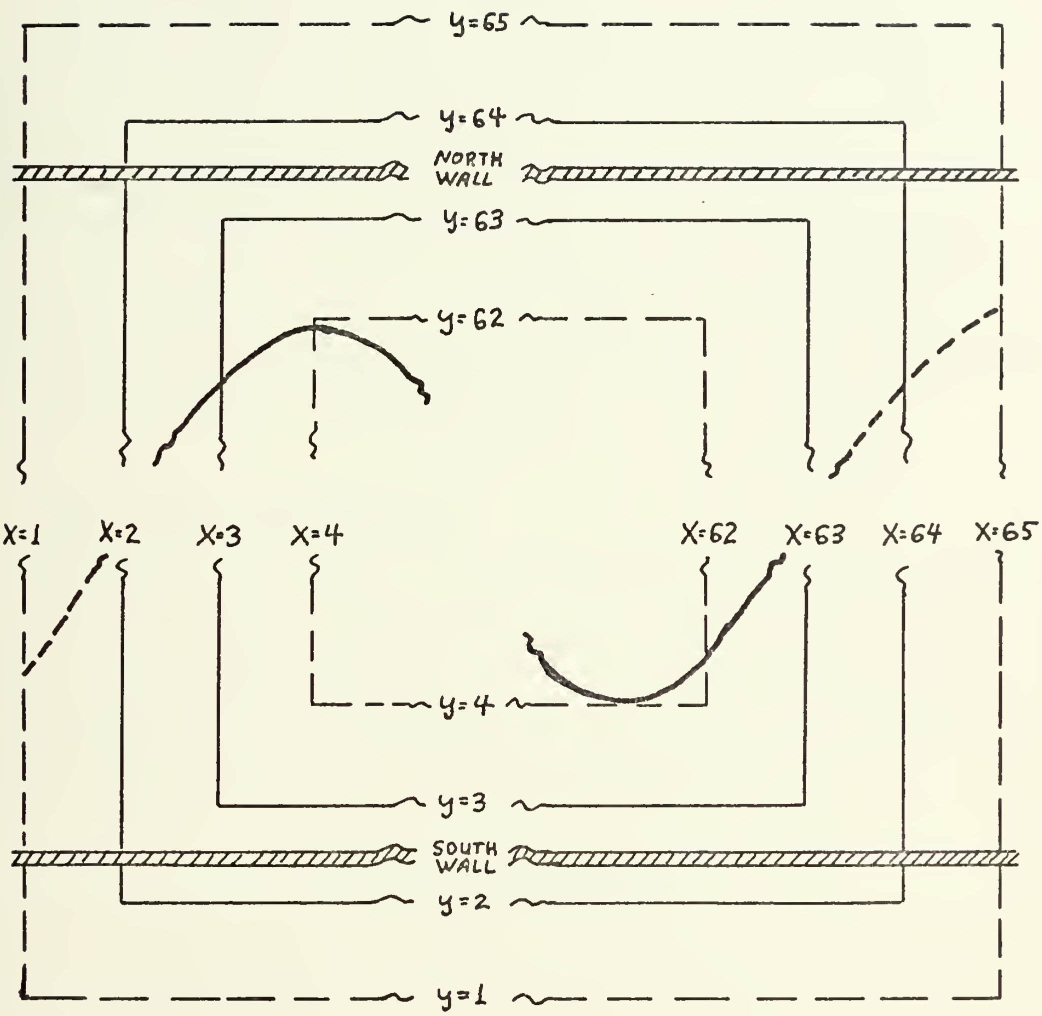

Illustrating the 65x65 expansion of the grid in Fig. 1 in order to apply fourth order space differencing over the same area. The dimensionless symbols x and y are used for notation convenience.

Figure 2

IV. GRID

A. A PARTICULAR STREAM FUNCTION

A 63x63 square grid as in Fig. 1 and as modified in Fig. 2 for fourth order space differencing is used to minimize the number of changes required to adapt programs to the FNWC 63x63 hemispheric grid. The boundaries in latitude extend from 30 to 90 degrees. Grid length is determined by dividing the geographic distance represented by this latitude difference into 62 equal parts.

B. FNWC 63x63 HEMISPHERIC

In conjunction with the actual 500 millibar data, the FNWC 63x63 hemispheric grid is used. This is a square representation of a hemispheric polar stereographic grid in which the grid distance d is determined by

$$d = \frac{d'}{m} = d'/\left(\frac{1 + \sin 60^{\circ}}{1 + \sin \gamma}\right)$$

where m is the map factor, d' is the grid distance at 60° latitude (381 kilometers), and $\sin \gamma$ is defined by

$$\sin \gamma = \frac{973.71 - R^2}{973.71 + R^2} \quad \text{where } R^2 = (I-I_p)^2 + (J-J_p)^2$$

I,J = arbitrary grid point.

I_p, J_p = grid point for the north pole = 32,32.

V. INITIAL CONDITIONS

A. A PARTICULAR STREAM FUNCTION

In order to obtain a smooth initial stream function field, an analytic solution to the nondivergent barotropic vorticity equation is used, namely

$$\psi = \psi_o \sin \frac{\pi}{L_y} (y - \frac{d}{2}) \cos \frac{2\pi}{L_x} (x-ct)$$

where c is the phase speed and the wavelength in the x direction and the half wavelength in the y direction are equal to 61d ($L_x = L_y = 61d$). The initial stream function is

$$\psi = \psi_o \sin \frac{\pi}{L_y} (y - \frac{d}{2}) \cos \frac{2\pi}{L_x} x .$$

Here, ψ_o is determined by using the relation

$$\psi_o \approx \frac{v_o L_x}{2\pi}$$

where v_o is the initial specified amplitude of the meridional wind speed derived from

$$v = \frac{\partial \psi}{\partial x} = \frac{2\pi}{L_x} \psi_o [\sin \frac{\pi}{L_y} (y- \frac{d}{2}) \cos \frac{2\pi}{L_x} x].$$

Using the initial field thus obtained, the linear balance equation

$$\nabla^2 \phi = f \nabla^2 \psi + \nabla f \cdot \nabla \psi$$

which in finite difference form may be written

$$\nabla^2 \phi_{ij} = f_{ij} \nabla^2 \psi_{ij} + \frac{1}{4} [\nabla_x f \ \nabla_x \psi + \nabla_y f \ \nabla_y \psi] \equiv F_{ij}$$

where

$$\nabla^2(\ ) = (\ )_{i+1,j} + (\ )_{i-1,j} + (\ )_{i,j+1} + (\ )_{i,j-1} - 4(\ )_{ij}$$

$$\nabla_x = (\ )_{i+1,j} - (\ )_{i-1,j} \text{ etc.}$$

The preceding equation may now be solved as a Poisson equation for the geopotential field. Thus,

$$\nabla^2\phi_{ij} = F_{ij}$$

The initial guess for the relaxation procedure is

$\phi_o = \bar{f}\ \psi_o$ where $\bar{f}$ is a mean coriolis parameter.

Subsequent "guesses" are made according to the relation

$$\phi^{(n+1)} = \phi^{(n)} + R_{ij}^{(n)}$$

where

$$R_{ij}^{(n)} = \alpha(\nabla^2\phi_{ij}^{(n)} - F_{ij})$$

and α is a relaxation coefficient.

Using $h = \phi/g$, computations for the initial height field are completed. Additionally, a constant height is added to each grid point value in order to eliminate negative heights, which would otherwise cause computational instability. (See Fig. 3)

B. ACTUAL 500 MILLIBAR DATA

The initial height field is obtained from the FNWC 500 millibar analysis. The linear balance equation is solved for the stream function as a Poisson equation using $\psi = \phi/\bar{f}$ as a first guess.

Differencing Scheme	RMSE For Position (Nautical Miles)	RMSE For Central Height (Meters)
Leap Frog	97	30
Leap Frog Fourth Order Space	76	31
Runge Kutta	93	31
Euler Backward	88	25

Table of root mean square errors in position and central height of the three low centers at 24, 48, and 72 hours as forecast by various differencing schemes (on actual data) in comparison to the corresponding analysis.

TABLE 1

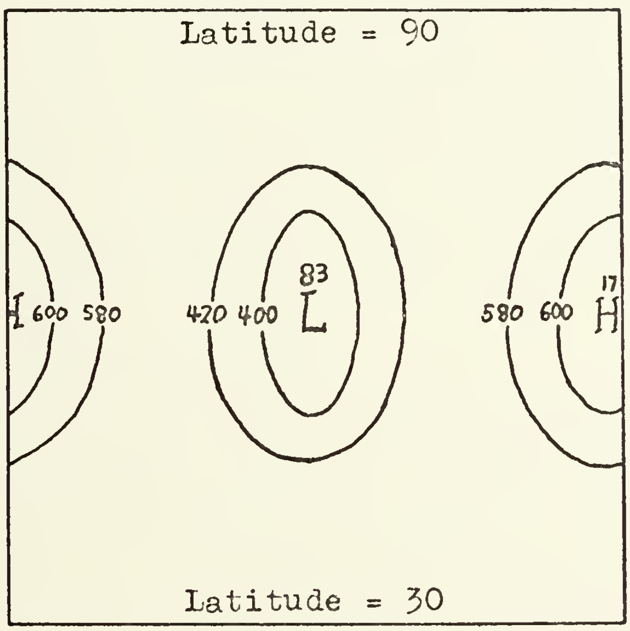

Initial height field as produced by a particular analytic stream function on a 63x63 grid. Only the central contours of the three features are illustrated.

Figure 3

VI. RESULTS

The results shown in the following figures were obtained from the computer subroutine mapping of the 63x63 height field obtained by the various differencing schemes using 10 minute time steps. One grid squares are used in the figures simply as a convenience to provide a ready reference scale to compare positions of low centers.

A. PARTICULAR STREAM FUNCTION

Results for the forecasts made using a particular stream function for the initial values are summarized in Fig. 4 for central height and relative position. The forecast results for the individual differencing schemes are presented in greater detail in Fig. 8 through Fig. 12.

B. ACTUAL 500 MILLIBAR DATA

The results of forecasts made on three low systems from the 500 millibar FNWC analysis are summarized in Fig. 5, Fig. 6 and Fig. 7. Although only low systems are illustrated in this study, similar results were obtained from the movement and intensification of highs. The time frame of this study begins with the 1200Z March 24, 1966 500 millibar heights and terminates with the 1200Z March 27, 1966 forecast. Low number one (See Fig. 5) was located over central Siberia. Low number two (See Fig. 6) and low number three (See Fig. 7) were located over Southwestern

Canada and Labrador respectively. Root mean square error computations for position and central height as forecast by each differencing scheme when compared to the corresponding analysis are contained in Table 1.

C. COMPUTER REQUIREMENTS

Although peak program efficiency was not attempted during the application of the various numerical schemes, consistency in application was carefully maintained. Using the leap frog scheme as a standard, the leap frog fourth order space differencing and Euler backward schemes require approximately a 35 percent increase in run time. The Runge Kutta scheme requires approximately a 170 percent increase in run time and a 25 percent increase in computer storage.

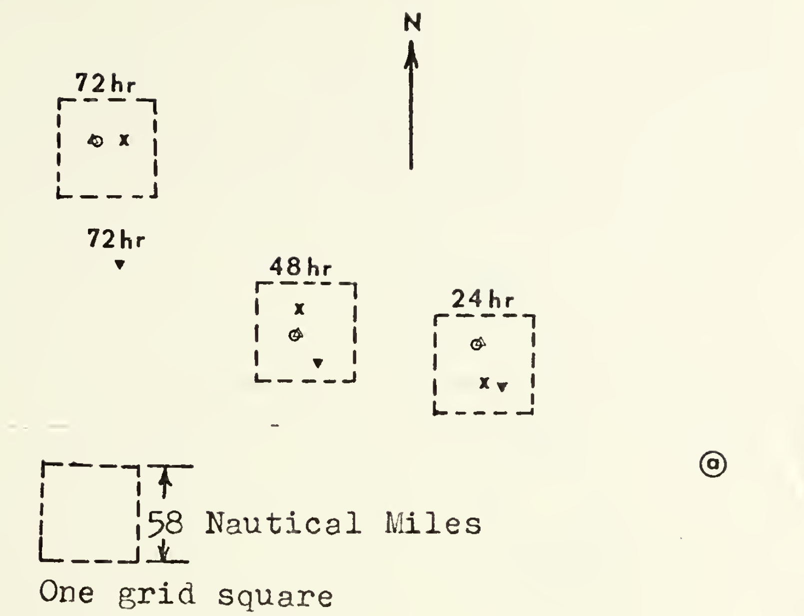

Differencing Scheme Forecast	Central 24 hr.	Height 48 hr.	(Meters) 72 hr.
x Leap Frog	382	383	383
o Leap Frog Fourth Order Space	383	384	383
△ Runge Kutta	382	383	380
▼ Euler Backward	383	384	385

◎ Initial Central Height --- 383 Meters

Relative position and central height of a particular stream function feature as forecast by various differencing schemes.

Figure 4

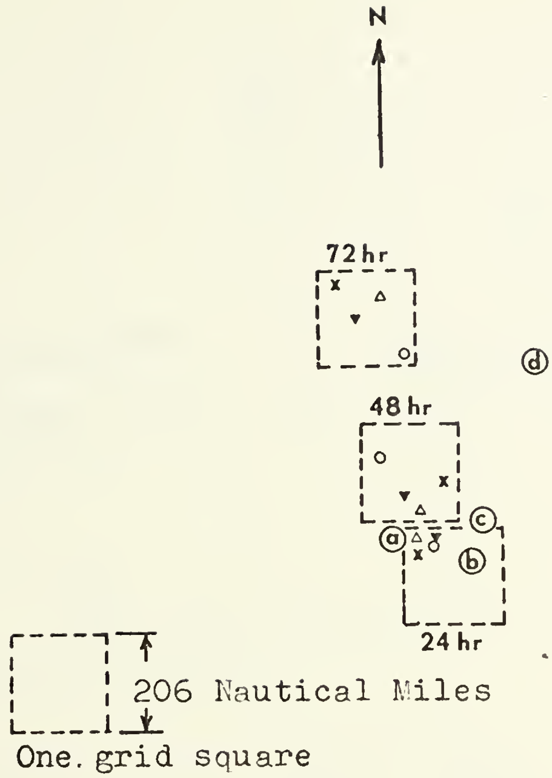

Differencing Scheme Forecast	Central 24 hr.	Height 48 hr.	(Meters) 72 hr.
x Leap Frog	4930	4940	4990
o Leap Frog Fourth Order Space	4940	4960	5030
▽ Runge Kutta	4930	4940	4990
▼ Euler Backward	4940	4940	4990
Corresponding FNWC Analysis	(b) 5020	(c) 5090	(d) 5110
(a) Initial Height FNWC Analysis		5040	

Forecast and analyzed relative positions and central heights for an actual data 500 millibar feature designated low number one.

Figure 5

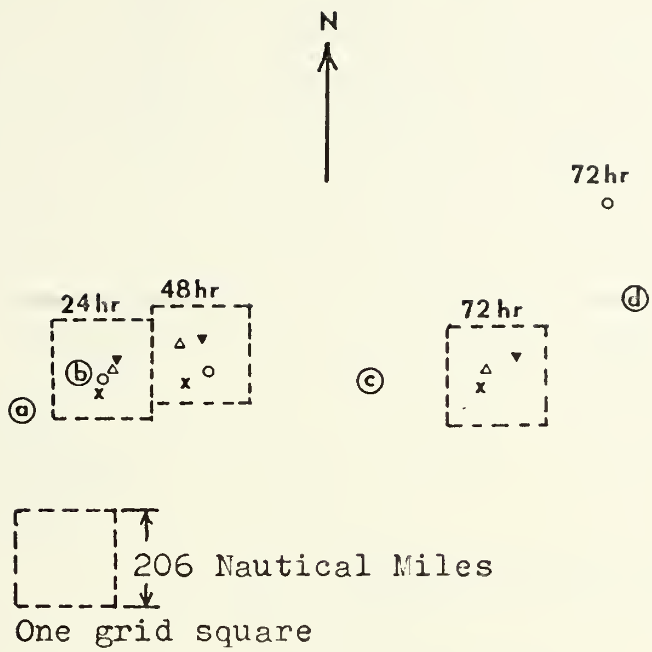

Differencing Scheme Forecast	Central 24 hr.	Height 48 hr.	(Meters) 72 hr.
x Leap Frog	5020	5070	5080
o Leap Frog Fourth Order Space	5060	5080	5050
△ Runge Kutta	5020	5080	5060
▼ Euler Backward	5020	5080	5080
Corresponding FNWC Analysis	b 5020	c 5120	d 5160
a Initial Height FNWC Analysis	5100		

Forecast and analyzed relative positions and central heights for an actual data 500 millibar feature designated low number two.

Figure 6

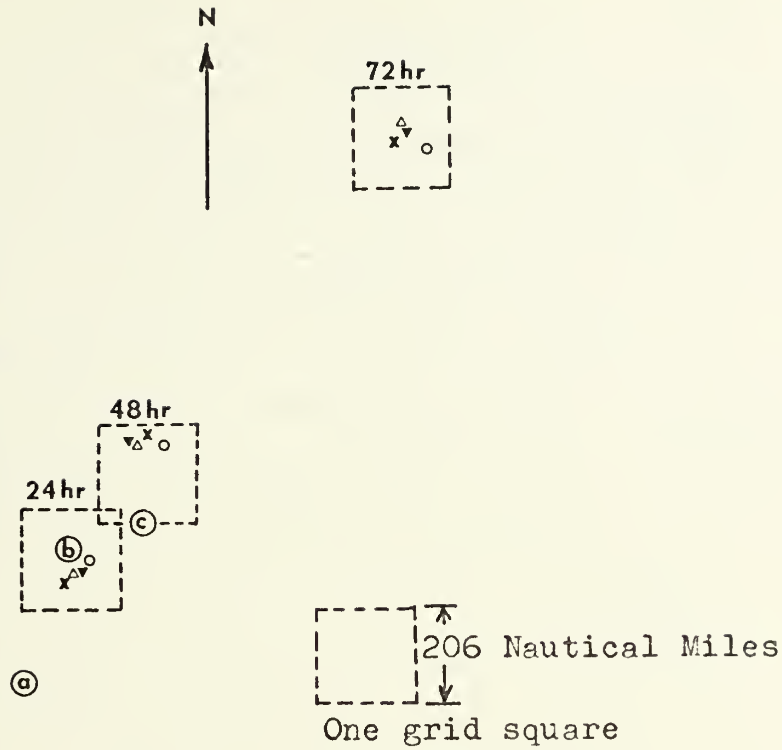

Differencing Scheme Forecast	Central 24 hr.	Height 48 hr.	(Meters) 72 hr.
x Leap Frog	4960	4960	4910
o Leap Frog Fourth Order Space	4960	4980	4960
△ Runge Kutta	4960	4950	4920
▼ Euler Backward	4960	4960	4930
Corresponding FNWC Analysis	(b) 4960	(c) 5110	(d) Filled
(a) Initial Height FNWC Analysis	4990		

Forecast and analyzed relative positions and central heights for an actual data 500 millibar feature designated low number three.

Figure 7

VII. CONCLUSIONS

The various differencing schemes were applied to the smooth analytic solution in order that differences in forecasts produced by these schemes would be more readily distinguishable than with actual data. However, the choice as to resolution was probably too high in this study (61 grid lengths per wavelength) and shorter wavelengths are yet to be tested. Differences produced in location and central values were not conclusive when compared to the results produced using actual data. A reduction in resolution for the analytic initial field (approximately six grid lengths per wavelength) would possibly produce a more meaningful separation in the accuracy produced by the various schemes.

The negligible increase in accuracy (four percent based on a root mean square error comparison) of the Runge Kutta scheme over the leap frog scheme does not justify the extremely large increase in computer time and moderate increase in computer storage. Both the leap frog fourth order space and Euler backward differencing schemes show promise for improved accuracy with a moderate increase in computer run time (approximately 35 percent). The leap frog fourth order space differencing scheme gave a 24 percent increase in position accuracy. The Euler backward scheme produced a nine percent increase in position accur-

acy and a 17 percent increase in central height. With both the Euler backward and the leap frog fourth order space schemes, the 35 percent increase in computer time could be reduced somewhat by more efficient programs. The small statistical sample of pressure systems examined in this study does not permit firm conclusions to be drawn regarding the various schemes tested. However, there is reason to believe that the fourth order space differencing of the nonlinear advection terms will reduce the phase error in the prediction of pressure systems and this method should be tested further. Williams [2] has shown that the pressure force need only be differenced with second order accuracy which permits a somewhat larger time step without computational instability than when fourth order differences are used throughout.

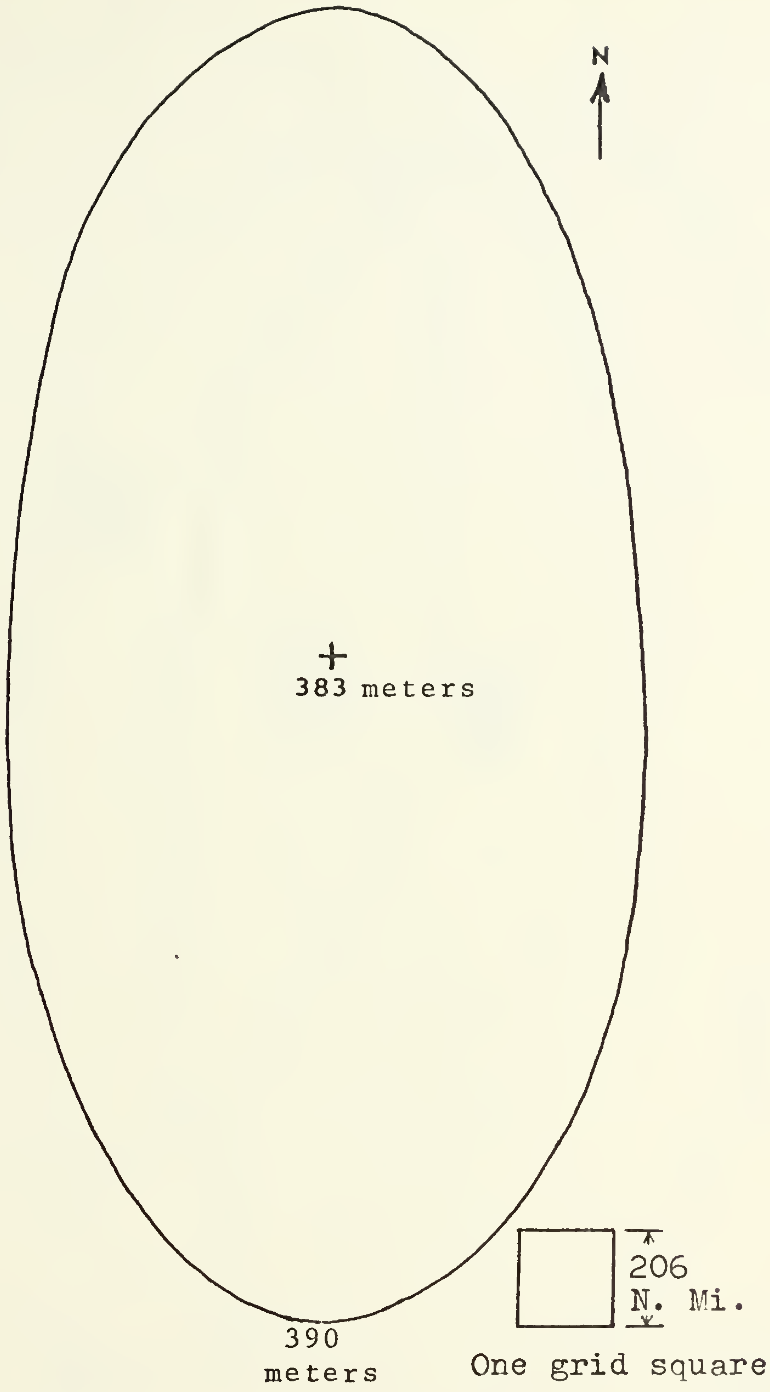

One feature in an initial height field produced from a particular stream function illustrating the central height and 390 meter contour.

Figure 8

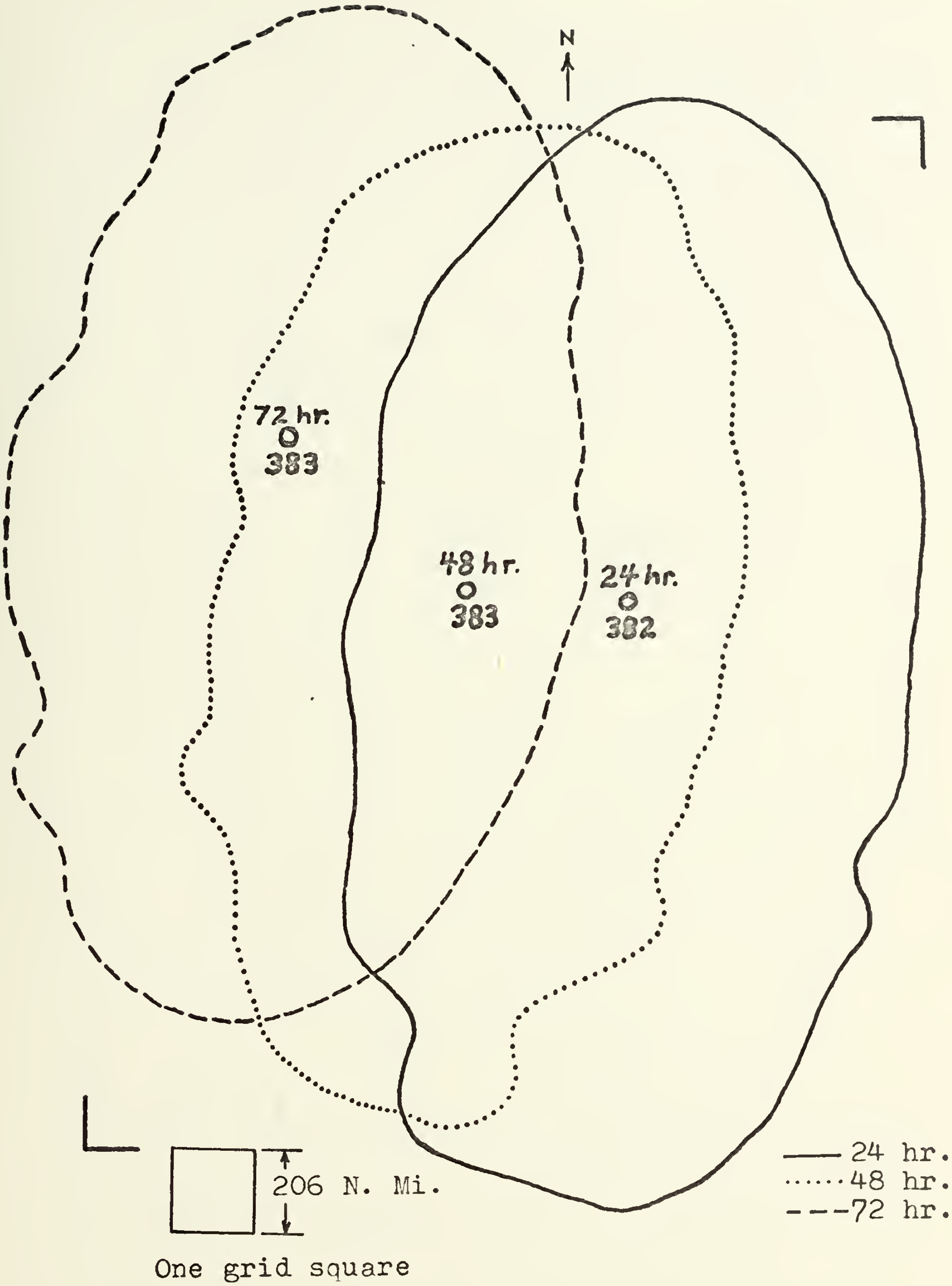

Forecast height in meters of central values and positions of centers and 390 meter contours for a particular stream function by the leap frog scheme.

Figure 9

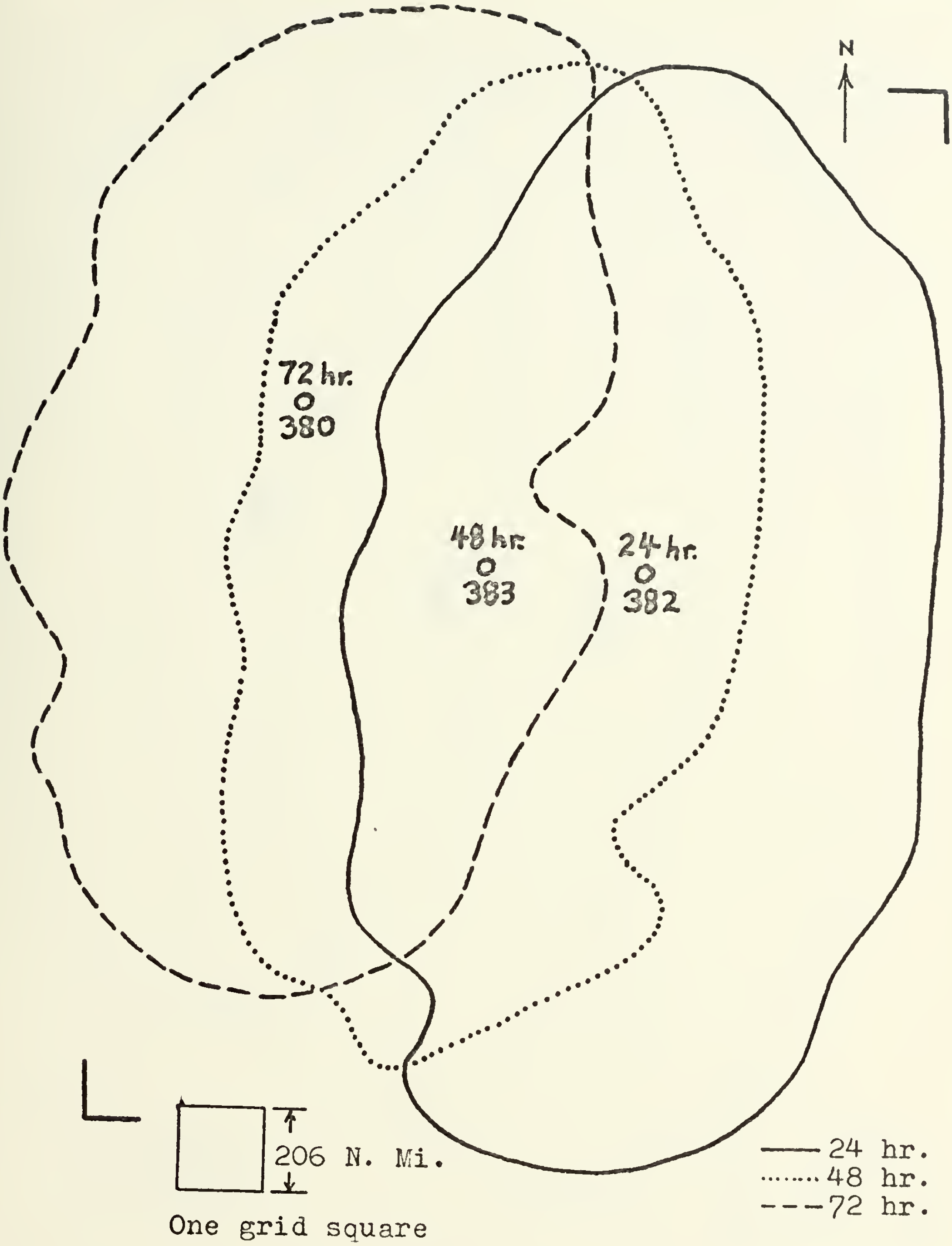

Forecast height in meters of central values and positions of centers and 390 meter contours for a particular stream function by the Runge Kutta scheme.

Figure 10

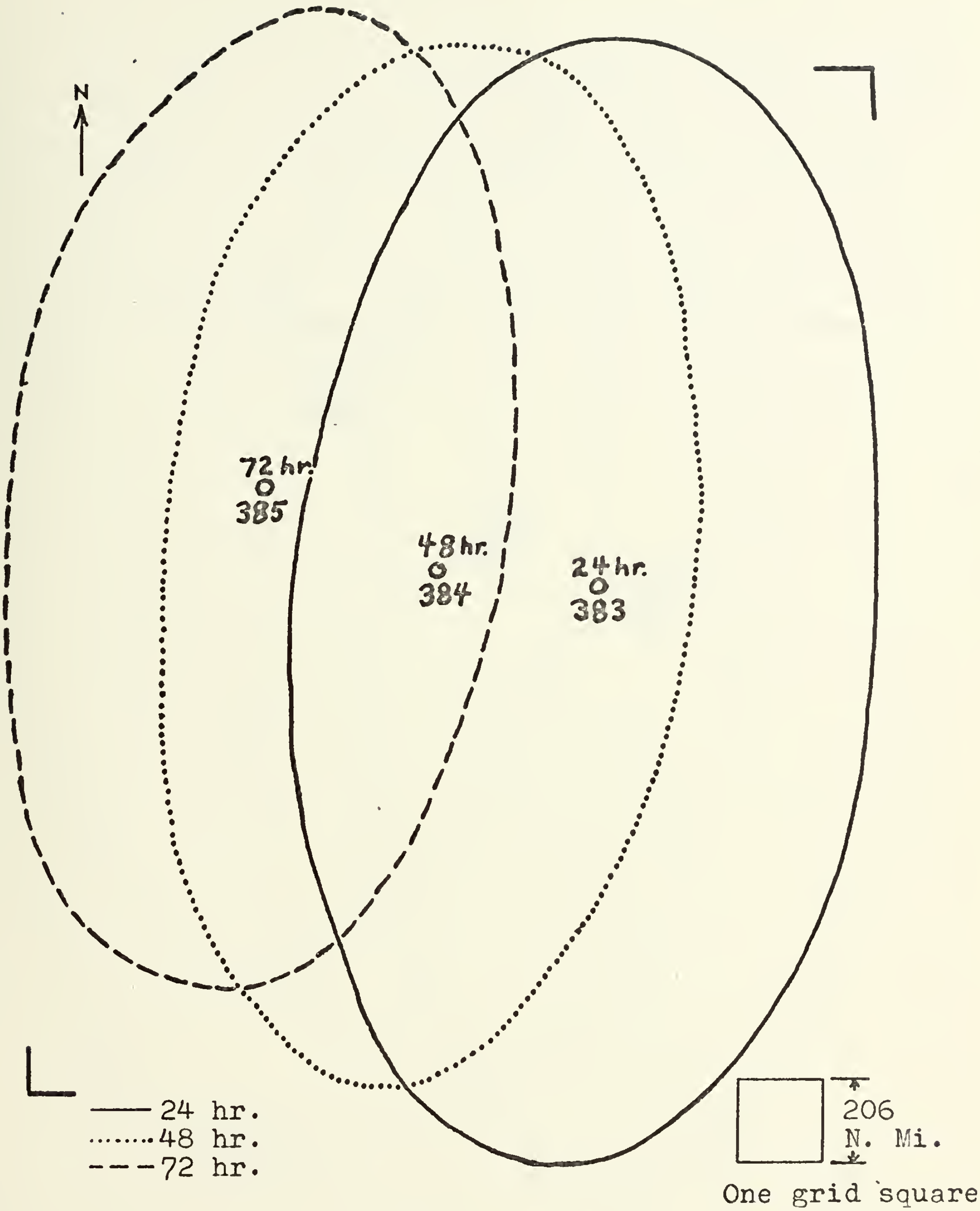

Forecast height in meters of central values and positions of centers and 390 meter contours for a particular stream function by the Euler backward scheme.

Figure 11

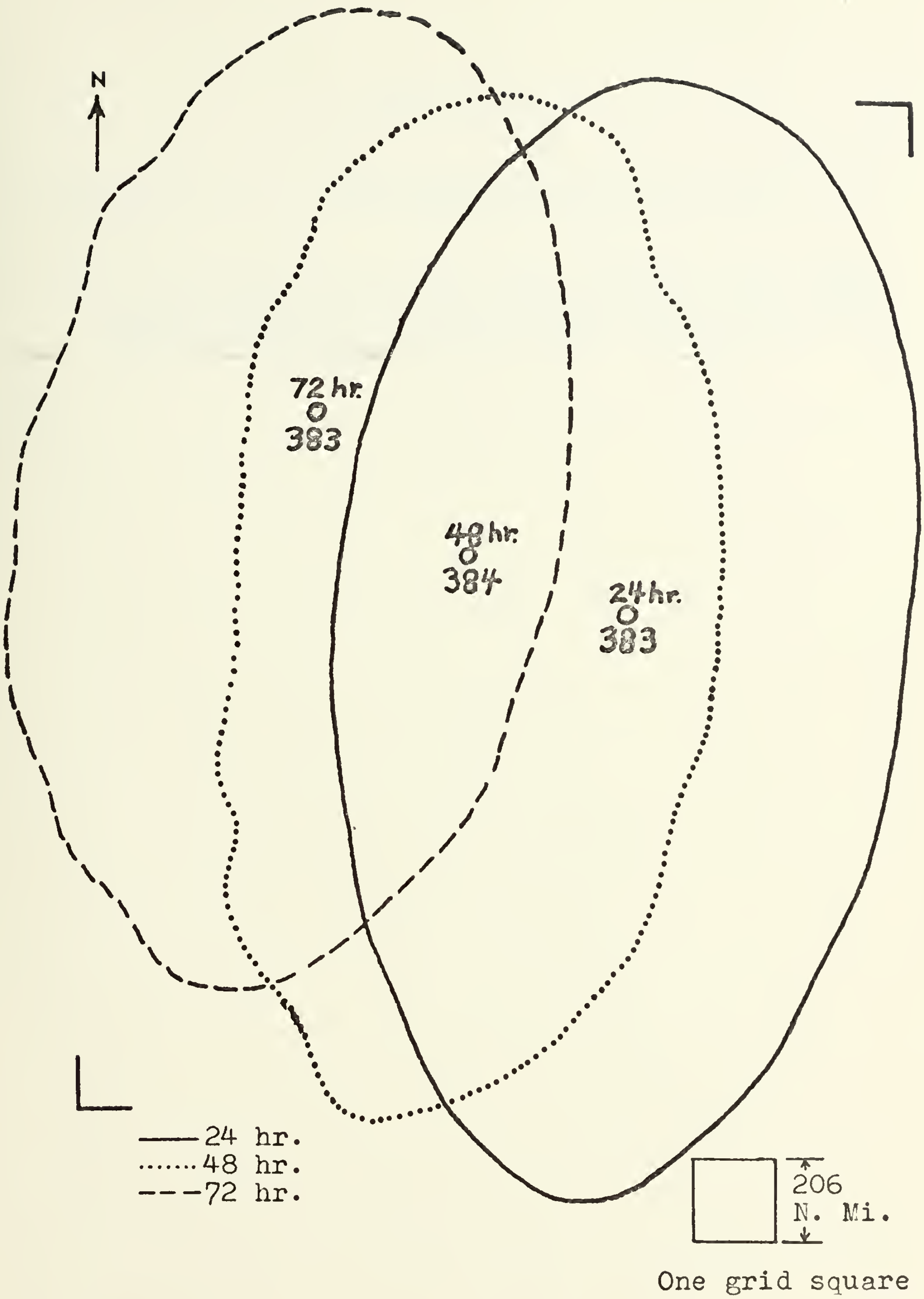

Forecast height in meters of central values and positions of centers and 390 meter contours for a particular stream function by the leap frog fourth order space differencing.

Figure 12

BIBLIOGRAPHY

1. Haltiner, G. J., Numerical Weather Prediction, Wiley, 1971.

2. Naval Postgraduate School Report 51Wu72031A, Phase Speed Errors with Second and Fourth Order Space Differences with Staggered and Unstaggered Grids, by R. T. Williams, March 1972.

INITIAL DISTRIBUTION LIST

		No. Copies
1.	Defense Documentation Center Cameron Station Alexandria, Virginia 22314	2
2.	Library, Code 0212 Naval Postgraduate School Monterey, California 93940	2
3.	Professor G. J. Haltiner, Code 51Ha Department of Meteorology Naval Postgraduate School Monterey, California 93940	5
4.	Lieutenant Commander J. R. Slaughter Carrier Airborne Early Warning Training Squadron 110 (RVAW-110) Naval Air Station, North Island San Diego, California 92135	2
5.	Department of Meteorology Naval Postgraduate School Monterey, California 93940	3
6.	Naval Weather Service Command Washington Navy Yard Washington, D. C. 20390	1

Security Classification

DOCUMENT CONTROL DATA - R & D

(Security classification of title, body of abstract and indexing annotation must be entered when the overall report is classified)

1. ORIGINATING ACTIVITY (Corporate author) Naval Postgraduate School Monterey, California 93940	2a. REPORT SECURITY CLASSIFICATION Unclassified 2b. GROUP

3. REPORT TITLE

Numerical Integration Experiments with a Barotropic Primitive Equation Model

4. DESCRIPTIVE NOTES (Type of report and inclusive dates)

Master's Thesis, March 1972

5. AUTHOR(S) (First name, middle initial, last name)

Jimmy R. Slaughter

6. REPORT DATE	7a. TOTAL NO. OF PAGES	7b. NO. OF REFS
March 1972	38	2

8a. CONTRACT OR GRANT NO. b. PROJECT NO. c. d.	9a. ORIGINATOR'S REPORT NUMBER(S) 9b. OTHER REPORT NO(S) (Any other numbers that may be assigned this report)

10. DISTRIBUTION STATEMENT

Approved for public release, distribution unlimited.

11. SUPPLEMENTARY NOTES	12. SPONSORING MILITARY ACTIVITY
	Naval Postgraduate School Monterey, California 93940

13. ABSTRACT

Experiments are carried out with various time and space differencing schemes applied to the barotropic primitive equations using both real data and a particular stream function which is an analytic solution to the nondivergent barotropic vorticity equation. With both types of data there were some significant differences in the forecasts produced by the various schemes. Replacement of the widely used leap frog (centered) scheme by others which eliminate or lessen some of its inherent errors at the expense of more computer time or storage appears to be justified at auch time when computer capacity no longer restricts operational use of these more time consuming schemes.

14. KEY WORDS	LINK A		LINK B		LINK C	
	ROLE	WT	ROLE	WT	ROLE	WT
barotropic primitive equations						
numerical forecast						

Thesis 134270
S57025 Slaughter
c.1
Numerical integration experiments with a barotropic primitive equation model.